ARMY RESEARCH LABORATORY

Subsurface Optical Microscopy of Coarse Grain Spinels Phase 1

by Donovan Harris

ARL-TR-6732 **December 2013**

NOTICES

Disclaimers

The findings in this report are not to be construed as an official Department of the Army position unless so designated by other authorized documents.

Citation of manufacturer’s or trade names does not constitute an official endorsement or approval of the use thereof.

Destroy this report when it is no longer needed. Do not return it to the originator.

Army Research Laboratory
Aberdeen Proving Ground, MD 21005-5069

ARL-TR-6732 **December 2013**

Subsurface Optical Microscopy of Coarse Grain Spinels Phase 1

Donovan Harris
Weapons and Materials Research Directorate, ARL

REPORT DOCUMENTATION PAGE	Form Approved OMB No. 0704-0188

1. REPORT DATE *(DD-MM-YYYY)*	2. REPORT TYPE	3. DATES COVERED (From - To)
December 2013	Interim	April 2010–July 2012

4. TITLE AND SUBTITLE
Subsurface Optical Microscopy of Coarse Grain Spinels Phase 1

5a. CONTRACT NUMBER

5b. GRANT NUMBER

5c. PROGRAM ELEMENT NUMBER

6. AUTHOR(S)
Donovan Harris

5d. PROJECT NUMBER

5e. TASK NUMBER

5f. WORK UNIT NUMBER

7. PERFORMING ORGANIZATION NAME(S) AND ADDRESS(ES)
U.S. Army Research Laboratory
ATTN: RDRL-WMM-E
Aberdeen Proving Ground, MD 21005-5069

8. PERFORMING ORGANIZATION REPORT NUMBER
ARL-TR-6732

9. SPONSORING/MONITORING AGENCY NAME(S) AND ADDRESS(ES)

10. SPONSOR/MONITOR'S ACRONYM(S)

11. SPONSOR/MONITOR'S REPORT NUMBER(S)

12. DISTRIBUTION/AVAILABILITY STATEMENT
Approved for public release; distribution is unlimited.

13. SUPPLEMENTARY NOTES

14. ABSTRACT
This is an interim report summarizing efforts to investigate the use of bioscience software applications to expand the use of optical microscopy in developing improved methods and procedures to document the subsurface structure of coarse grain transparent ceramic materials in situ. The approach was to evaluate commercial software modules normally used by the life sciences using coarse grain magnesium aluminate (MgAl2O4), and aluminum oxy nitride (AlON). The microscope used is a hybrid system possessing transmitted and reflected light illumination capabilities for both laser and broadband light sources and both confocal and widefield capabilities. The 6–13-mm-thick samples produced some unexpected optical responses while exploring the available contrasting/illuminating techniques of the hybrid system. Some of the limitations experienced using a 32 bit operating system and imaging applications are briefly noted. The less-than-ideal results observed in the video files derived from the Z-stack captures show the needed information was captured, just not reliably nor in a quantifiable format using the available technology.

15. SUBJECT TERMS
subsurface, optical microscopy, coarse grain, 3-D simulation

16. SECURITY CLASSIFICATION OF:			17. LIMITATION OF ABSTRACT	18. NUMBER OF PAGES	19a. NAME OF RESPONSIBLE PERSON
a. REPORT	b. ABSTRACT	c. THIS PAGE			Donovan Harris
Unclassified	Unclassified	Unclassified	UU	38	19b. TELEPHONE NUMBER (*Include area code*) 410-306-0707

Standard Form 298 (Rev. 8/98)
Prescribed by ANSI Std. Z39.18

Contents

List of Figures

List of Tables

1. Introduction

This is an interim report summarizing efforts to investigate the use of bioscience software applications to expand the use of optical microscopy in developing improved methods and procedures to document the subsurface structure of coarse grain transparent ceramic materials in situ. The approach was to evaluate different illumination and contrasting modes and the image processing results for coarse-grained magnesium aluminate ($MgAl_2O_4$), and aluminum oxy nitride (AlON). Presently, the documentation of ceramic internal structures rely on specimen etching and electron microscopy, which, while providing high-resolution images, does destroy an indeterminable amount of potentially significant features. The object is not to replace the electron microscopy technique but to supplement it so to better assess the mechanical test data and the modes of failure. The instrument used is a hybrid Zeiss Pascal 5 confocal microscope, which will be referred as "Z1m." The unit possesses transmitted and reflected light illumination capabilities for both laser and broadband light sources. The confocal capability does not work with the coarse-grained spinel. The Zeiss Pascal software, here after referred to as "LSM," cannot correctly setup or process Z-stacks using the digital camera, and third party application such as the National Institutes of Health's (NIH's) freeware program Image J have issues with the camera-generated 1388 × 1080 pixel images.

In an attempt to resolve the LSM constraints, Zeiss's widefield application, AxioVision 4.x (AV4), was added to the same controller/analyzer computer. Both Zeiss 32 bit applications require the same configuration application, creating compatibility issues. The current installation of AxioVision, AV4, is not reliable for image generation and processing. Specifically the 32 bit AV4 will generate files too large to store uncorrupted, be processed or allow the export of uncorrupted image files. Excellent images, 3-D images, and Z-stack videos are regularly generated, but just not reliably. Those successes have prompted the acquisition of a new broadband widefield Zeiss Z2m with a 64 bit computer system, and upgrading the current 32 bit AxioVision license to a
64 bit license.

This report first presents background discussions of the microscope, supporting software, Z-stacks, and widefield broadband illumination, then summarizes laser imaging and broadband imaging efforts, and concludes with pending issues. Other possibly relevant issues and a deeper background are intentionally ignored to maintain a narrowly focused scope until project completion.

2. Background

While executing several concurrent material improvement programs, the current etch and electron microscope method to determine internal microstructure of transparent ceramics proved too inefficient and not as effective as required. The required etching process takes too long to generate statistically viable data within program deadlines. The inability to document or estimate the etching losses and to accurately control the etch depth raises accuracy and reliability questions. Being a destructive method, comparing pre- and post-test structures is not possible. With the grain boundaries of tested and etched samples, it is not always possible to distinguish between test damage and etching damage. A nondestructive in situ imaging technique is needed to document internal structure before and after testing, such as four or three point bend tests.

The objective is the development of procedures suitable for a technician to perform, with the two-fold purpose of better documenting grain, void, and inclusions differences and relationships through the thickness prior to and post mechanical testing, and improving the nondestructive analysis of internal structural differences and relationships between similar materials 2–13 mm thick.

This project required an initial investigation of all available optical microscopy contrasting modes. Techniques to identify possible methods were under taken using a hybrid Zeiss Pascal 5 confocal microscope, to be referred to as “Z1m” hereafter and the Pascal 5 application software, as “LSM.” Existing spinel, $MgAl_2O_4$, and AlON samples provide the evaluation test samples. The Z1m system has both coherent and broadband illumination for reflected light and transmitted light techniques (see figures 1–3). There are three photomultipliers, two for confocal/reflected coherent light, and one for nonconfocal, transmitted coherent light. A high-resolution monochrome digital camera supports all broadband imaging, with the hybrid LSM software supporting all four sensors. The transmitted laser capability and the digital camera are nonstandard capabilities and not documented beyond two radio buttons in the LSM configuration panel. The lasers cannot be used to image using the camera, and the photomultipliers cannot support non-scanning illumination. The inability to upgrade the Z1m and LSM software to correct working issues prompted the installation of Zeiss’s AV4 software in four phases. Both the LSM and the AV4 use the same configuration application and have generational and compatibility issues. A new Z2m broadband system with an AV4 upgrade to 64 bits will replace the existing systems to address these and other issues.

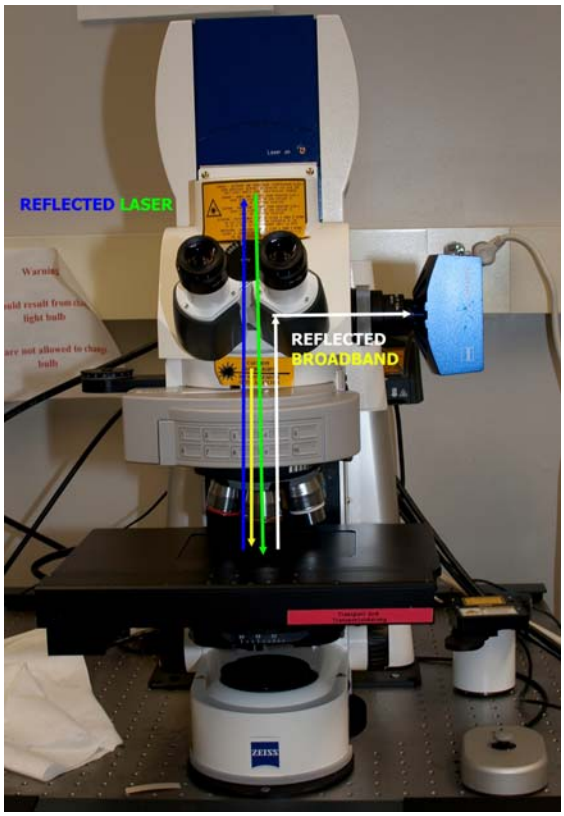

Figure 1. The reflected light paths of the Z1m system. The large unit at the top houses both the laser light pipe illuminators and the confocal working elements of the system.

Figure 2. A portion of the transmitted light paths. The photo tube detector of the transmitted laser path is hidden by the stage.

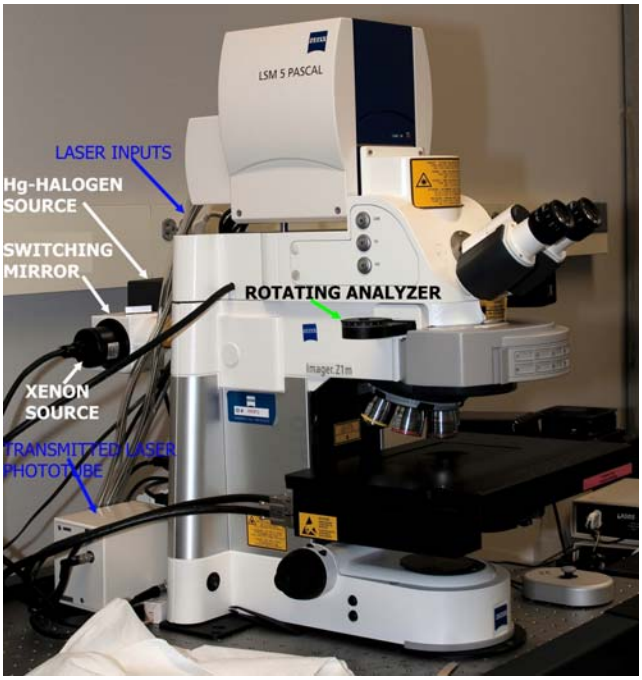

Figure 3. The transmitted laser detector, the rotating polarization analyzer, and other components obscured in figures 1 and 2.

3. Z-Stacks and Slices

Z-stacks are a series of images taken at successfully deeper focal points along the Z-axis at the same magnification. Both the LSM and AV4 applications have the capacity to generate Z-stacks, using different functional algorithms. In the LSM application, wavelength, pinhole size, and numerical aperture are the adjustable variables used to generating the appropriate slice spacing independent of sample thickness, which determines the number of slices collected. The LSM default spacing for the camera is 1 µm, independent of the objective used. For the existing AV4 configuration, the only adjustable variable appears to be the objective/numerical aperture and presumes broadband illumination and is also independent of sample thickness. Both Zeiss applications LSM and AV4 processing algorithms require equally spaced slices. The 50× and the 100× objectives, NA = 0.95, both generate slices 0.41 µm apart but have differing working distances of 270 and 230 µm, respectively.

Table 1 lists the default AV4 Z-stack imaging parameters for the microscope system used. The LSM Z-stack parameters allow variable slice spacing, which are not readily presented in table form.

The present operational issues, to be discussed later, have affected only the in situ studies and not the extended focus capabilities for other studies as demonstrated by figures 4–6. Figure 4 is a portion of a ballistic impact spall crater at 25×, generated using 24 slices and presenting an image around 2400 um deep according to table 1, which was derived from the AV4× metadata. An illustration of the AV4 three extended-focus processing algorithms results appears in figure 5, done at 50× using reflected darkfield. The same Z-stack file was the source for all three images. A 200× detail study of a spall fragment surface, figure 6, illustrates the limits of using reflected-darkfield illumination.

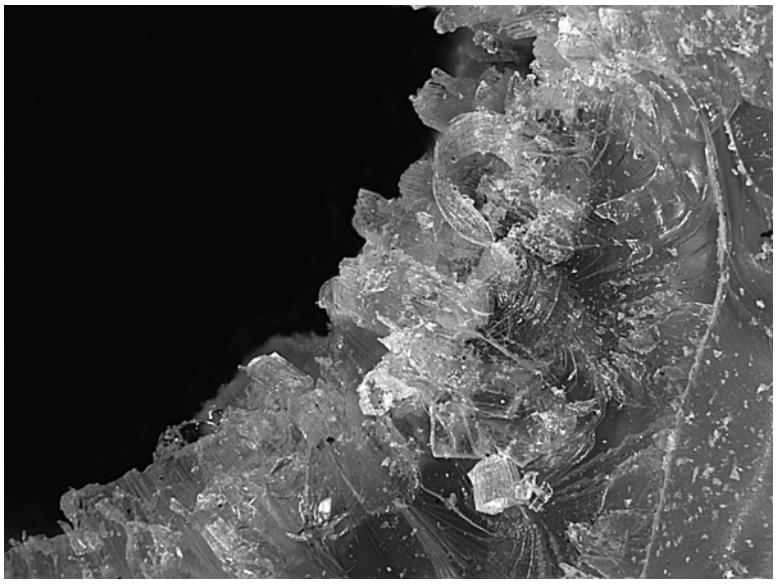

Figure 4. A 25×, 24 slice simulation of a portion of a spall creator as viewed from the exit face toward the strike face. The AV4× calculated depth of view is 2408 um.

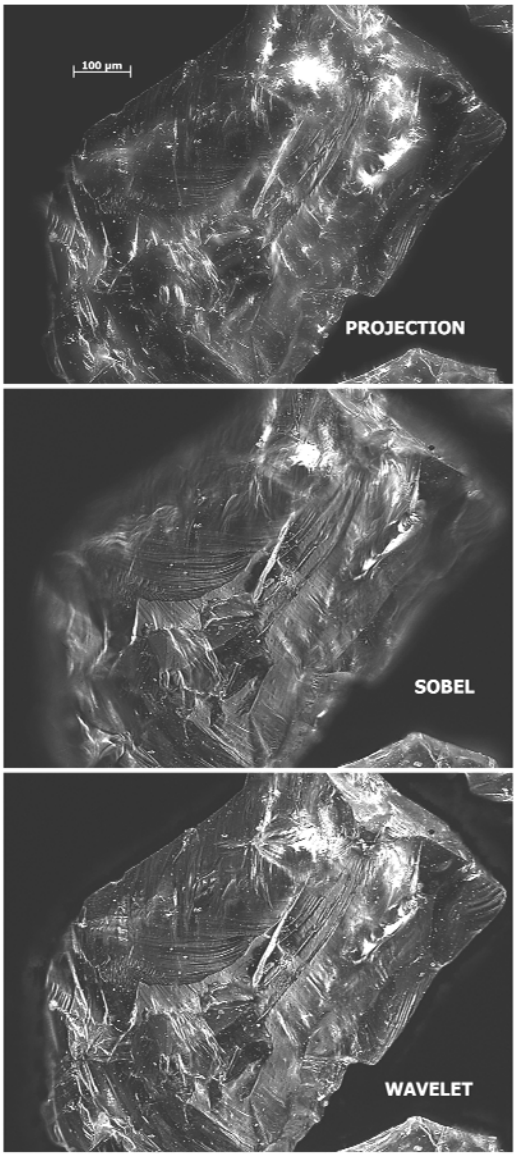

Figure 5. The results of the three topographic processing algorithms for a single Z-stack file.

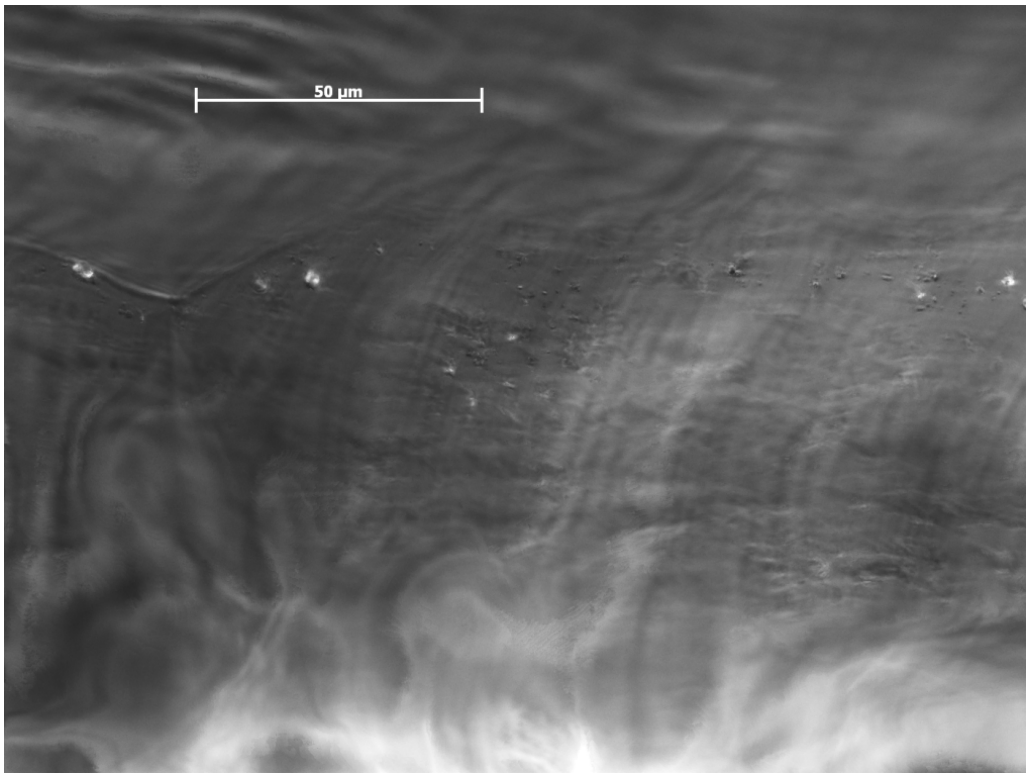

Figure 6. A fragment surface captured at 200×. The transparency of the sample created issues for the processing algorithms, limiting the resolution of the entire image.

Table 1. Field of view resolutions and sizes.

Objective	**µm/pixel: AxioVision**	**µm/slice: AxioVision**	**Nominal Field of View: µm 1388 Pixels × 1040 Pixels**
02.5×	2.58	102	3581 × 2683
05×	1.29	22	1791 × 1342
10×	0.65	5.9	902 × 676
20×	0.32	1.47	444 × 333
50×	0.13	0.41	180 × 135
100×	0.06	0.41	83 × 62

4. Widefield Illumination

The light-sample interactions shown in this section appear to arise from the sizes of the grains, 200–500 µm. For the spinel samples, add, having grains optically isotropic, physically isometric, and although essentially cubic, an octahedral form that is most common. All the spinel imaging results demonstrate a crude lens system, which will randomly interact with the microscope optics. Only three AlON samples with equally large grains have been examined using only reflected darkfield, so any sample-microscope optics interactions are not known.

In figures 7 and 8, a narrow fracture remnant is illuminated by transmitted brightfield. The dual lens Koehler condenser, center bottom of figure 7, has a retractable top lens for objectives 10× and above. The features seen on and in the lens actually originate at the interior fracture face, as does the apparent surface roughness of the sample top surface. Disengaging the top condenser lens and lowering that unit widens the light field, as in figure 8. The Z-stacks images randomly contain illumination field width artifacts.

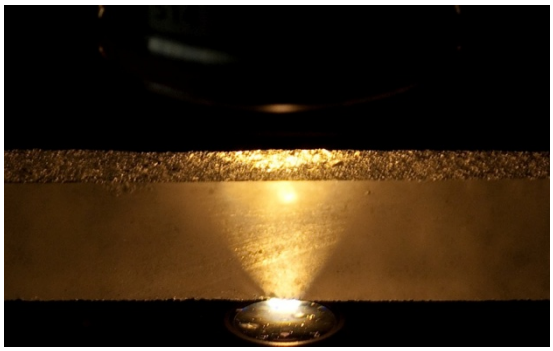

Figure 7. A spinel fracture fragment using transmitted illumination with a Koehler condenser. The apparent top surface roughness and lens defects originate on the interior portion of the far side fracture face.

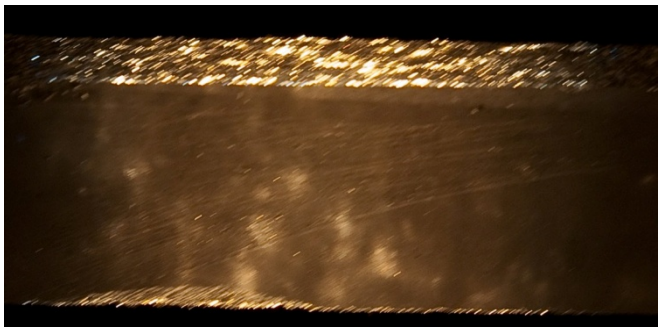

Figure 8. The effect of removing the lens at the bottom of figure 7 from the light path. The polished surface retains its rough appearance, while individual interior facets of the fracture face appear as white blobs. Both the grain coarseness and the isotropic nature of the spinel are responsible for the optical effects in figures 7 and 8.

Reflected brightfield illumination mimics its transmitted counterpart, figure 9, except the objective and brightfield cube controls the light field in place of the Koehler condenser.

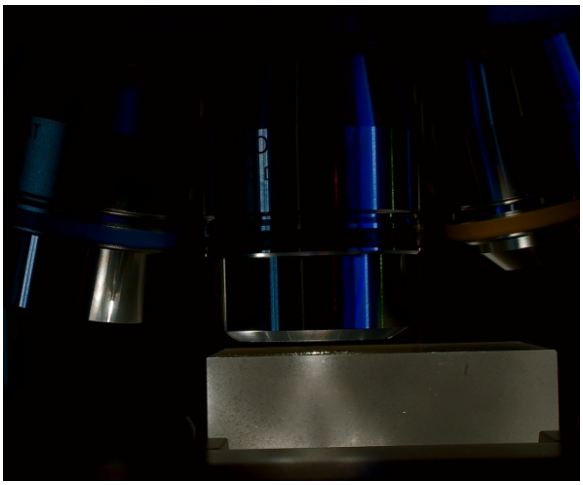

Figure 9. Demonstrates a slightly different set of effects when using reflected brightfield and a 20× objective with a different sample, figures 7 and 8. The light image seen on the near face originates mid sample and appeared on the left side face.

The 20× objective focused on the polished face-generated facing light pattern, with an identical pattern visible on the left face. The 5× objective using a HAL-100 source produced the three-disk effect seen in figure 10.

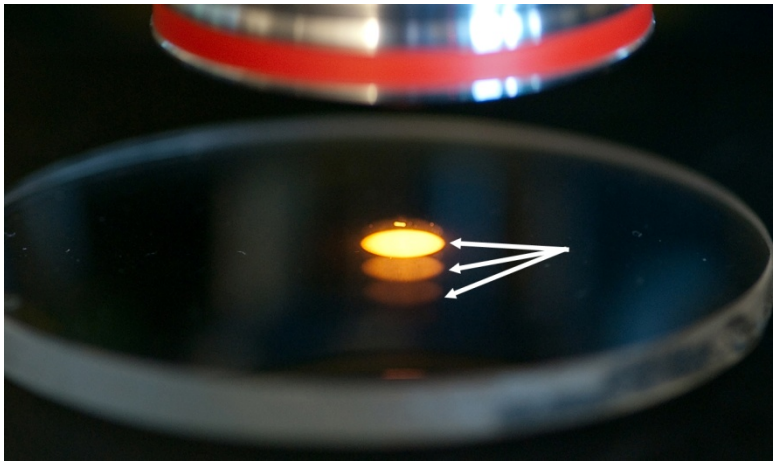

Figure 10. The interaction of the 5× objective with a 6-mm-thick spinel using reflected brightfield illumination at a low-voltage setting. The top and bottom discs of light appear to correspond with the two faces.

That same 6-mm-thick sample produced the 10× objective-HAL-100 patterns of figure 11.

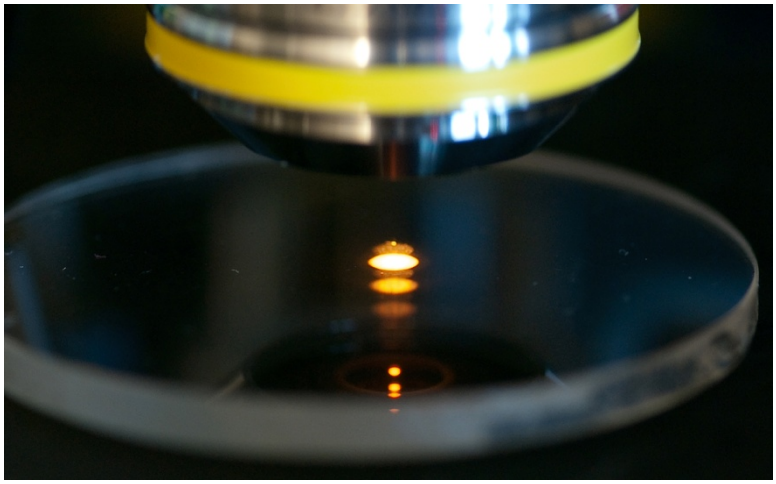

Figure 11. Similar to figure 10, the pattern becomes more complex with the 10× objective.

The effect of setting HAL-100 illumination to a higher voltage with the 10× objective generates a different response as demonstrated in figure 12.

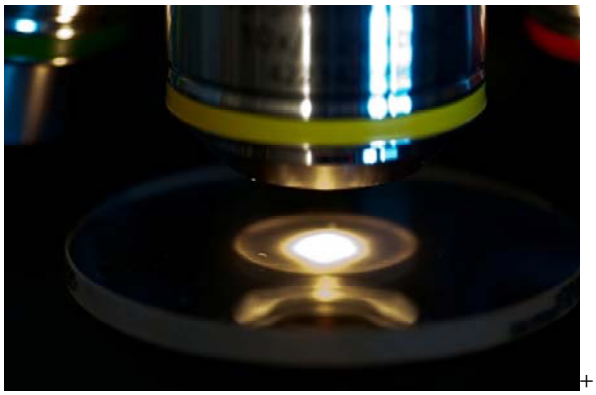

Figure 12. Figure 11 with the HAL-100 at a higher voltage.

In figure 13, an X-Cite 120 Q is the source for the 10× objective.

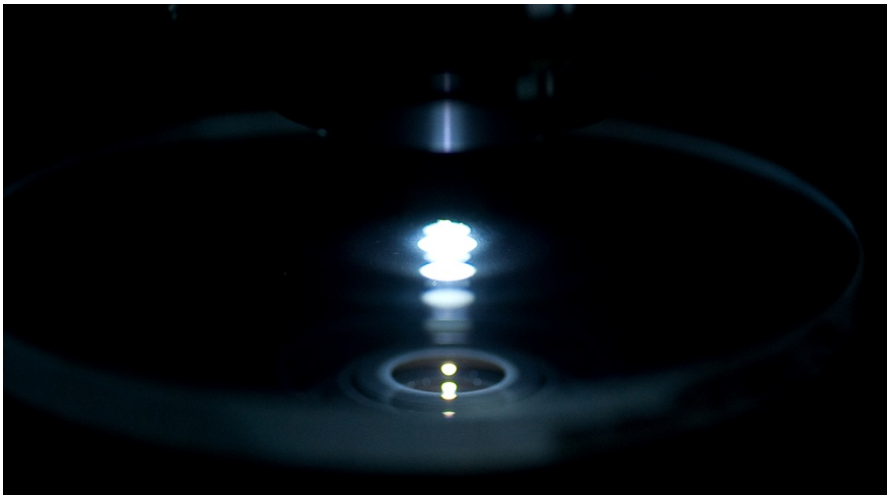

Figure 13. The effect of switching to the X-Cite 1200 source.

A different effect is visible with a sintered spinel X-Cite illuminated using the 2.5× objective as shown in figure 14. The 2.5× objective using X-Cite illumination generated the response in figure 15.

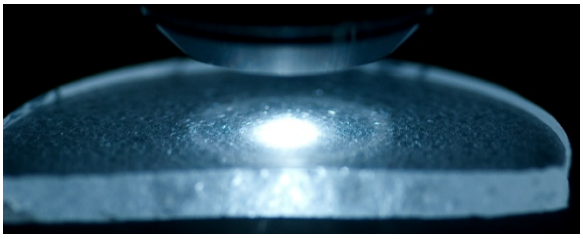

Figure 14. An image of a 6-mm-thick sintered spinel illuminate by the X-Cite source through the 2.5× objective.

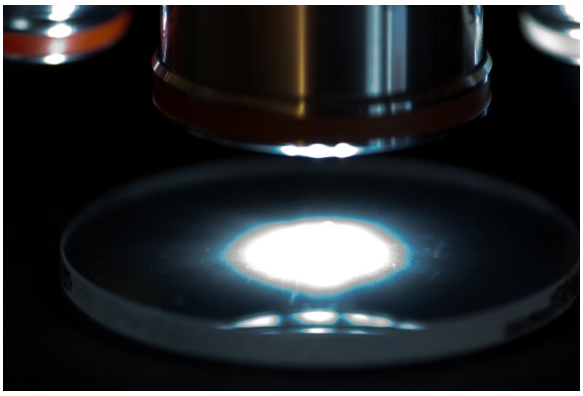

Figure 15. The sintered spinel is replaced with a hot-pressed and Hot Isostatic Pressing (HIP)-processed spinel sample.

HAL-100 darkfield illumination through a 2.5× objective generated the response in figure 16, whereas X-Cite illumination and a 10× objective created figure 17. In both figures, the active imaging area is centered in the dark disk. All the illumination images were generated ad hoc to help supplement written notes and promote a fuller understanding of the dynamics involved, as do some line-light side-illumination images from the same period.

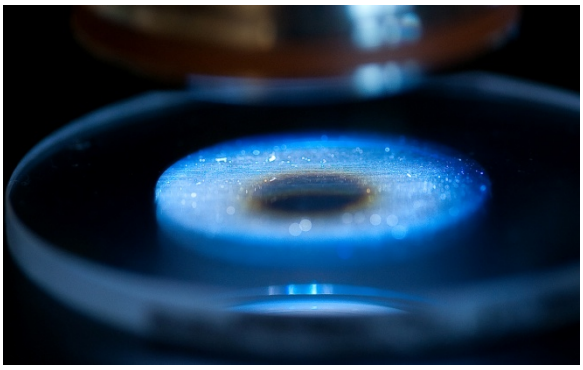

Figure 16. The figure 15 settings are changed to reflected darkfield and generated this response. The HAL-100 is the illumination source. Note that the dark center is the imaging area.

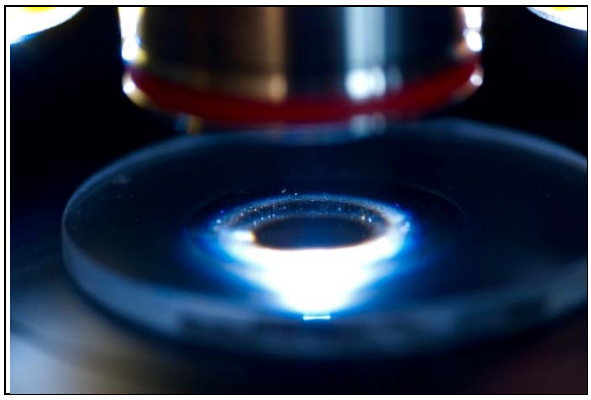

Figure 17. The X-Cite source was utilized, producing this dramatic effect and crisper Z-stack images.

Figures 18 and 19 are macro-images taken through the 10-mm-sample thickness, revealing grain-like structures on the far polished face only. A 456 nm LED line bar illuminated in figure 15 and a Xenon fiber optic bar illuminator is shown for figure 16. The optical in situ or subsurface imaging of coarse grain spinels and AlONs is optically more complex than expected. An overhead view of the side illumination field is shown in figure 20.

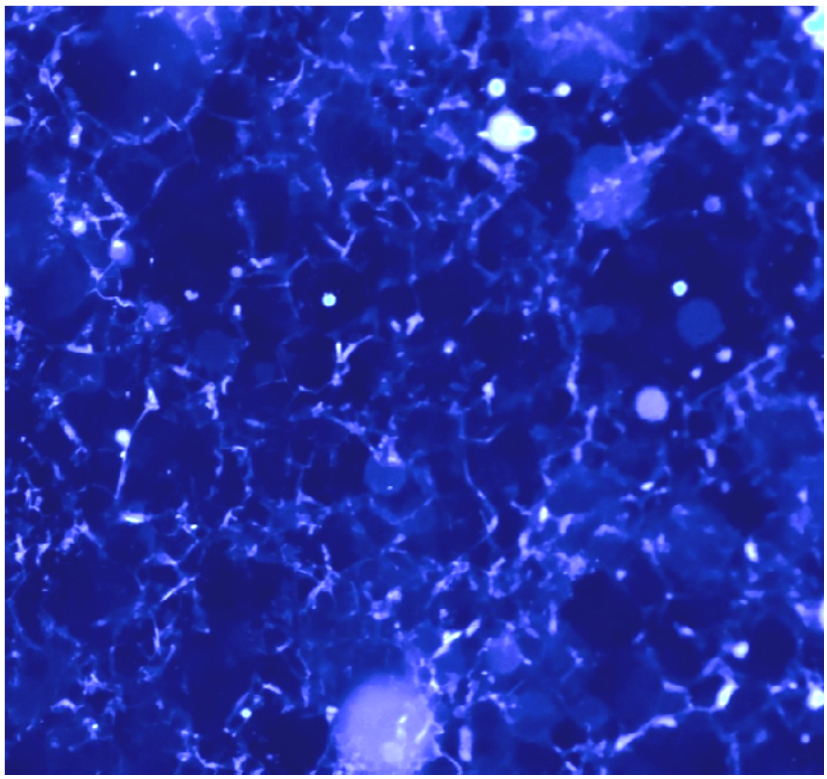

Figure 18. A 200 mm macro lens image of the far face image of a 10 mm thick spinel, using a 470 nm illumination source.

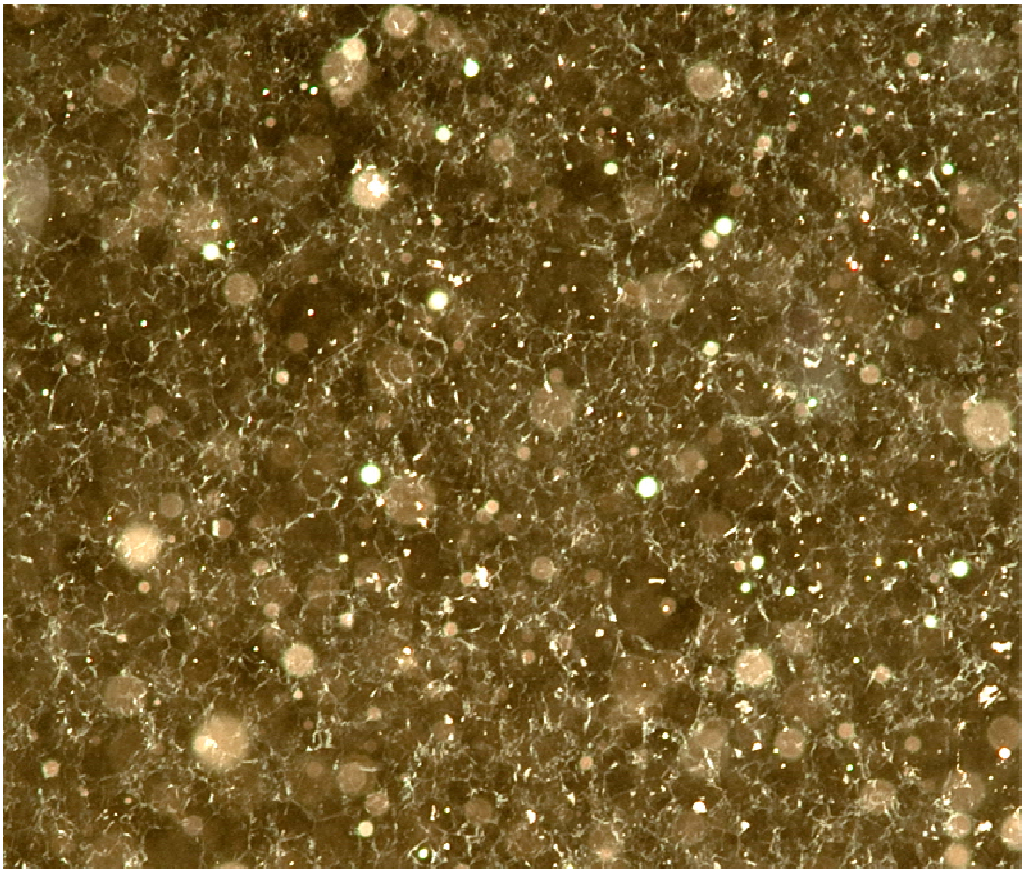

Figure 19. Taken with a 100 mm macro lens and an EKE Xenon source with fiber optics. Both figures 18 and 19 were illuminated from the side, through the sample.

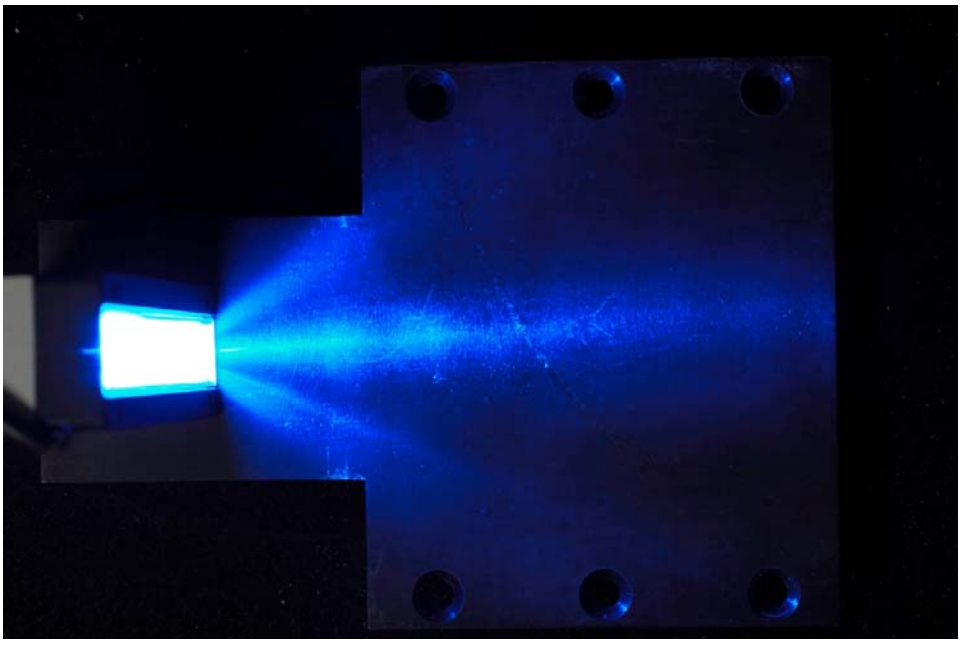

Figure 20. An overhead view of the illumination field for figures 18 and 19. The camera focused on the backface face of the sample, shooting across the light fields.

5. Coherent/Confocal Light Methods

The confocal capabilities seemed the natural choice to perform in situ studies. Five available wavelengths, 458, 488, 514, 543, and 633 nm, coupled with an adjustable pinhole size, provides a wide range of resolution options over a magnification range of 25× to 1000×. The LSM 5 Pascal confocal module, seen in figure 3, houses the emission fiber optics from the lasers, the photomultiplier detectors, dichroic beam splitters, emission filters, and laser beam scanning mirror. The scanning beams are focused in a diffraction limited mode using the objective (Zeiss).

The normal limitations include the working distance of the objective and the sample thickness. Our average grain sizes are between 300–400 µm, reducing the maximum usable magnification to 200× for samples 3 mm thick or less. The specimens studied range from 2 to 12.5 mm thick, with the largest population 10 mm thick. Independent of sample thickness, confocal imaging would not work. The efforts by several vendors' application laboratories using user-supplied samples produced identical results. Grain size appears to be the major factor, based upon the subsequent widefield studies discussed next.

Figure 21 shows the individual frames from one confocal Z-stack. Row 1 and row 2 together as shown is not to be expected, either makes sense by itself. Rows 5 and 6 repeat the problem that rows 1 and 2 have. Only rows 3 and 4 resemble a normal scan result, but they lay mid sample, where grain density appears the highest when using widefield techniques. In figure 22, clearly focused grain boundaries appear in plane with laser beam patterns, the latter being the usual indicator of a lack of focus. This can occur when the surface roughness value is approximately equal to the wave length, but only if working at 500× to 1000× and employing a small pin hole size. The magnification for figure 21 is 25×. The use of a solid opaque stage insert may have played a role similar to the one it manifested when using reflected widefield imaging.

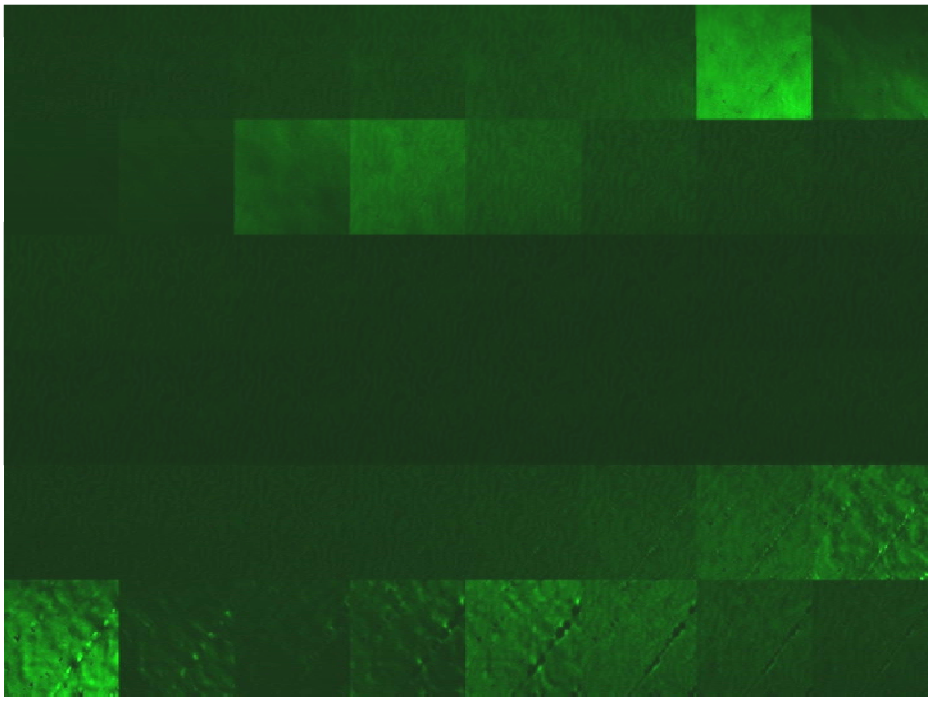

Figure 21. A confocal Z-stack gallery of a 6-mm-thick spinel. Although the individual rows could be normal for a confocal Z-stack, when taken together they are unintelligible.

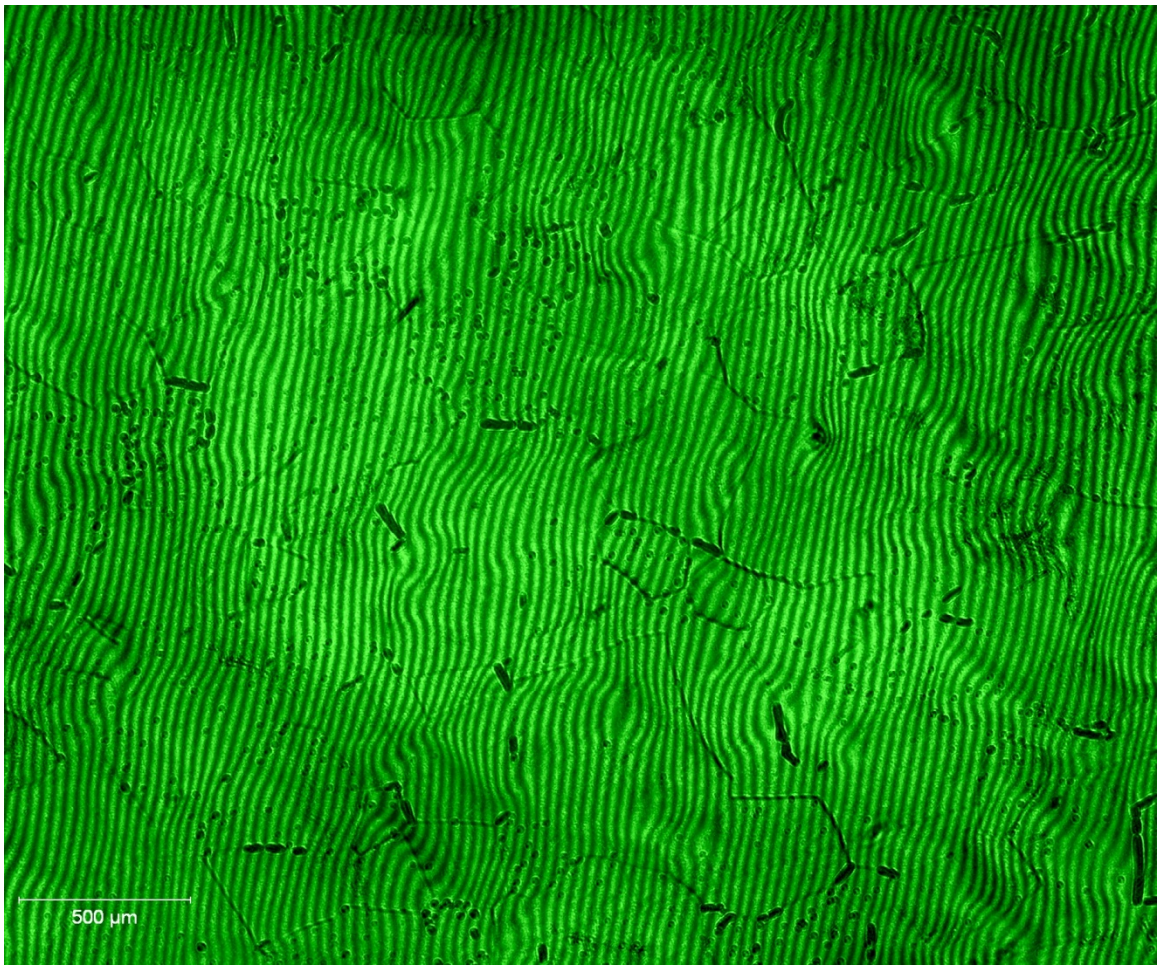

Figure 22. A single slice confocal image that appears both in and out of focus at the same points. At 500–1000×, this is seen in adjacent areas on flat surface using nanometer increments. This is a 50× image with a slice depth in the micron range.

Transmitted laser imaging proved to be moderately successful, generating reliably reproducible images, but possessing narrow, relatively flat gaussian histograms at 458 nm. Increasing the wavelength improves the histogram response, producing cleaner images at the expense of the smaller inclusions and thinner grain boundaries. Increasing sensor contrast during capture only increases image noise as does post processing to recapture those lost features. Issues with the confocal mode and imaging fluorescently tagged samples later revealed the laser sources to be misaligned in the confocal head unit. These studies will be repeated following removal of the AV4 application and restoration of the Z1m and the LSM configuration files to their pre-AV4 state.

6. Reflected Broadband

Both LSM and AV4 support the same broadband illumination techniques in both reflected and transmitted modes and are able to generate Z-stacks, but not at the same level of capability. The LSM camera capability presumes single shots, thus the Z-stack process is more cumbersome than in AV4, whereas actual camera control is better. The first series of reflected broadband studies used a LSM only system.

The Zeiss HRm camera is a discontinued 12 bit fiber optic unit, normally operating in 8 bit mode in LSM. In AV4, the camera while identified as a 14 bit firewire system, still used the hardcoded fiber optic parameters until operationally corrected. The fiber optic camera parameter file in the AV4 hardware configuration panel is viewable but not accessible. Using the camera parameters box in the "Live" panel and performing five re-entries, shut downs, and restarts embed the firewire parameters in the AV4 operating configuration, improving the AV4 camera control with more reliable file processing by the two AV4 three-dimensional (3-D) application modules. The camera configuration panel in the microscope configuration module still retains the original hardcoded parameters. Unfortunately, most of the existing AV4 data was generated using the hardcode parameters, and the LSM Z-stacks file format cannot be exported to AV4 without stripping off the metadata needed for processing.

Darkfield illumination produces the best results when using an X-Cite 120 Q illumination source, whereas the HAL-100, tungsten halogen, source generates a broader glare response. The other reflected light modes, brightfield, and circular differential interference contrast can generate anomalous results. In brightfield, it is possible to over-focus, generating a continuous Z-stack that images top down then bottom up, while continuing to focus downward. Over-focus tends to happen when using a solid opaque or glass stage insert. An opaque insert produces uniform images throughout the over-focused Z-stack, a glass insert increasingly noisier images. Except for darkfield, reflected light imaging can also generate the amorphous features in figures 23 and 24, which appear around 4–6 grain layers deep, then dissipate over the same distance and are not actually any part of the sample. A solid opaque stage insert supported the samples in figures 23 and 24, and figure 22. Using an open frame glass slide insert solves both problems, but at the cost of reduced contrast, especially samples 6 mm and thicker, through the Z-stack.

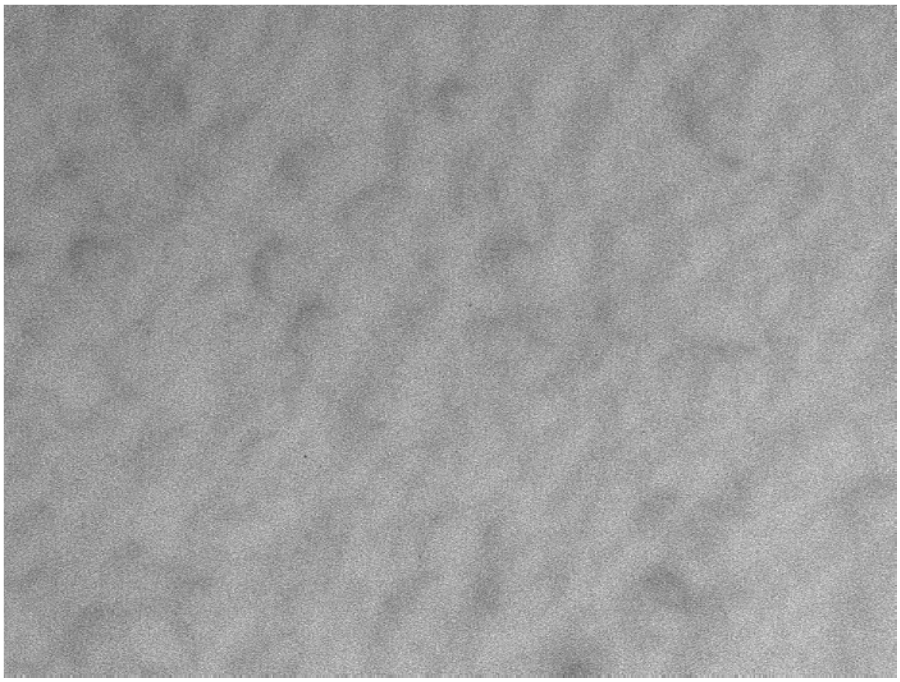

Figure 23. Captured around 1.2 mm deep into a 10-mm-thick sample. A variant of this image persisted for another 1 mm before clearing. One of the circular-differential interference contrast modes illuminated the sample. Removing the solid stage insert eliminated this effect.

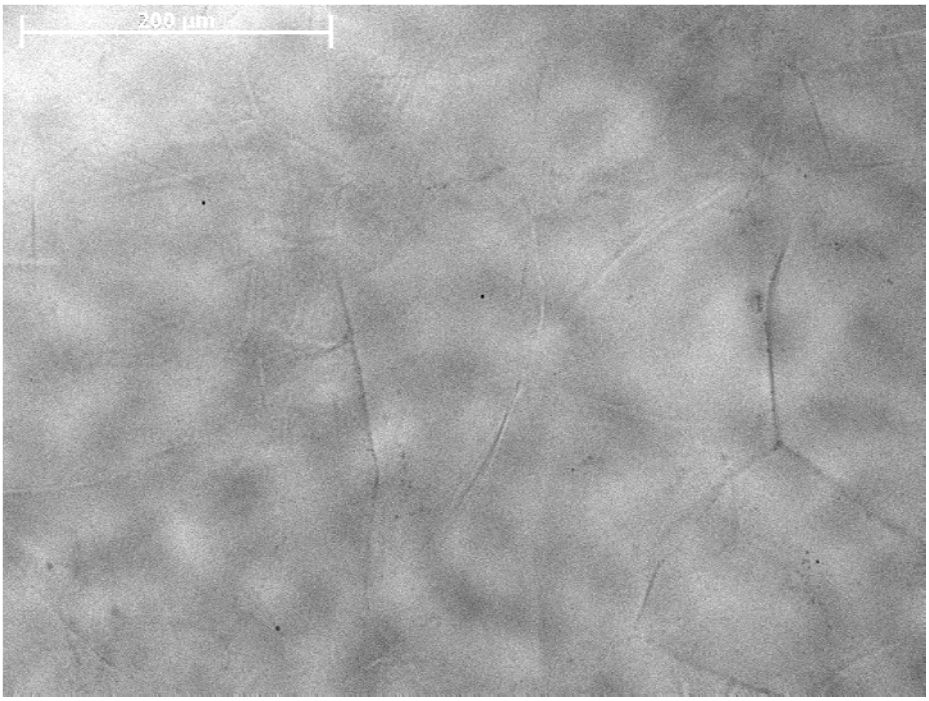

Figure 24. A variant of the effect in figure 22 in another sample at a deeper depth.

The AV4 stack-processing modules presume the imaging of a single surface as depicted in figures 25, 26, and 27. In situ imaging, figure 28 shows four focus images, involves intercepting multiple grain boundary interfaces down the Z-axis. The AV4 3-D topographic processing has a problem generating any type of surface using in situ grain boundaries; Image J-32 bit plug-ins can generate a simulation of the adjacent grain faces if the stack focus is centered mid grain for images 512 × 512 pixels. Extended focus or depth of field processing again assumes white/bright features of interest on a black/dark background, which works fairly well with reflected darkfield but not for other modes using the present software capabilities.

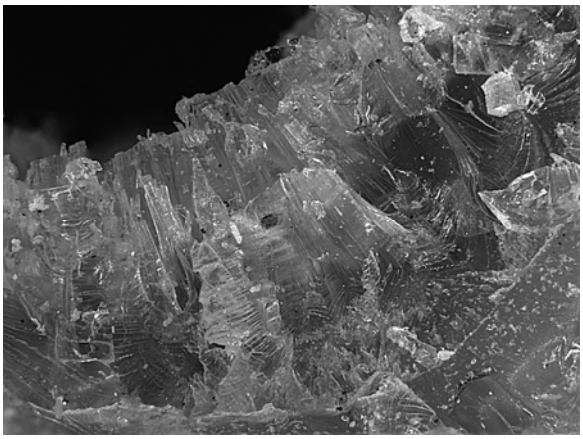

Figure 25. A different area from the figure 4 spall crater, again demonstrating that the AV 4× modules work well processing single surfaces.

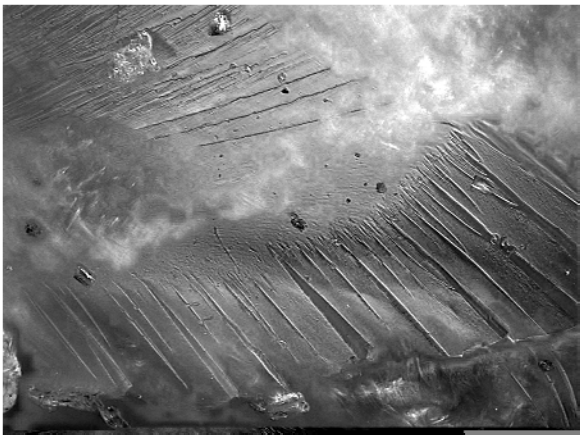

Figure 26. The spall crater from figures 4 and 25 closer to the exit face. Here the increased transparency in the sample and the absence of “black” region cause the processing some problems and reducing the sharpness seen in the earlier images.

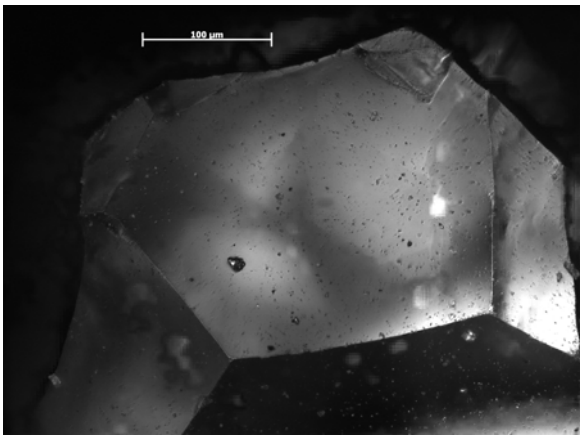

Figure 27. A darkfield image of spinel spall fragment. The internal light scatter and transparency of the grain generated problems for the processing algorithm. Although detail is generally good, each face is inconsistent in the rendering.

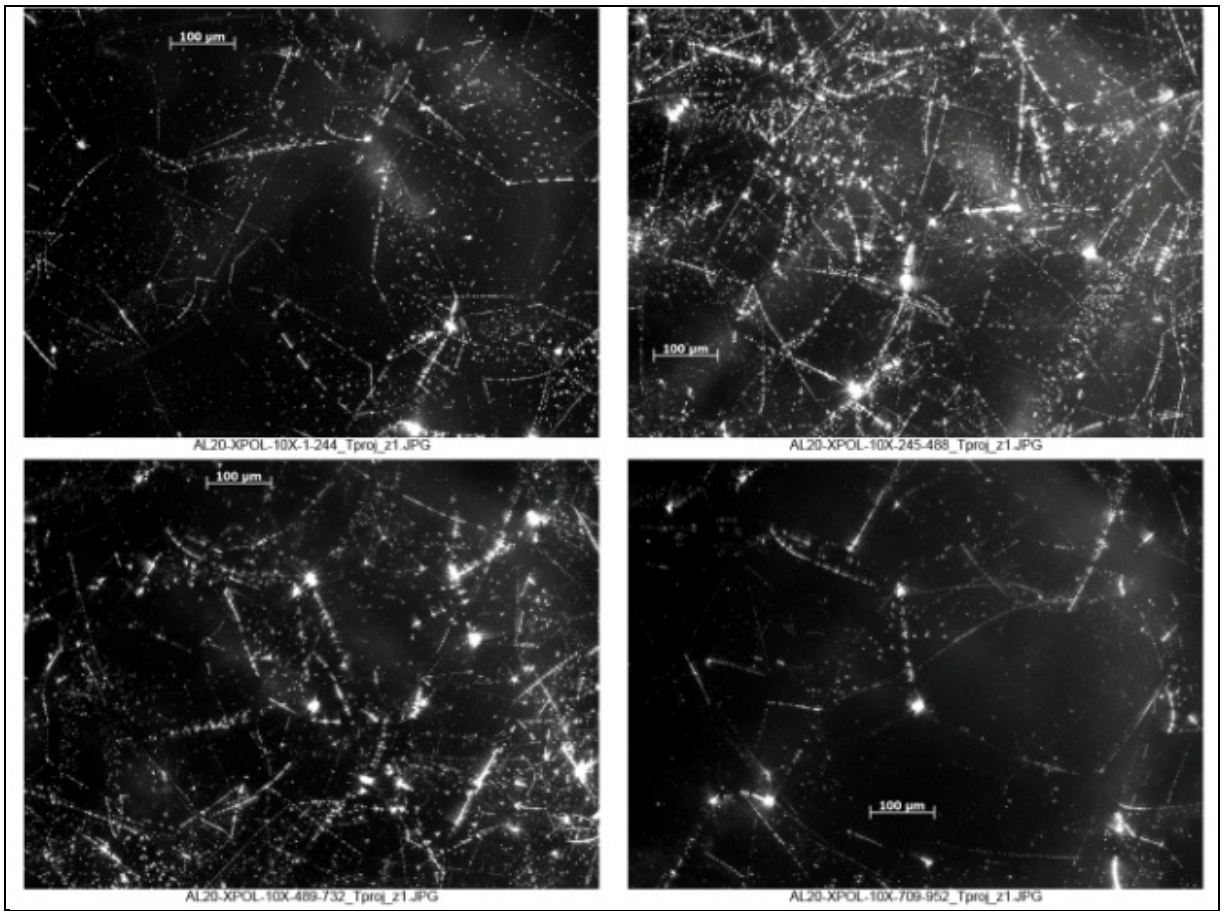

Figure 28. A darkfield set of images rendered from a single 952 slice Z-stack. Note the difference in density of the grain boundaries through the sample. The flaring along the boundaries and the general light pollution limit the utility of the reflected darkfield.

7. Transmitted Broadband Imaging

The Z1m objectives do not support phase imaging, and the system cubes only support Circular-Differential Interference Contrast (C-DIC) imaging in the reflected mode, whereas the Koehler condenser assembly is able to produce transmitted light illumination for brightfield, darkfield, C-DIC, and phase contrasting modes.

Polarized light is a brightfield variant, not supported by a monochrome camera, and degraded by the misaligned rotating analyzer. Cross-polarized light visually produces tight red and blue striped patches, whereas to the monochrome camera those patches are broad/diffuse light and dark patches obscuring grain boundaries and other features. An internal post protecting the camera prevents seating the rotating correctly; as a result, the analyzer partially blocks the optical path distorting the polarization field.

All the transmitted modes, broadband and coherent, produce images with dark gray or black grain boundaries against light gray backgrounds, figure 29, whereas the extended focus and 3-D topography applications are premised on dark backgrounds with white features of interest. Post processing using a color lookup table to invert the image, b/w to w/b, does not work, the two variants produce identical results. A separate application module providing live w/b capture capability will be a new capability with the Z2m.

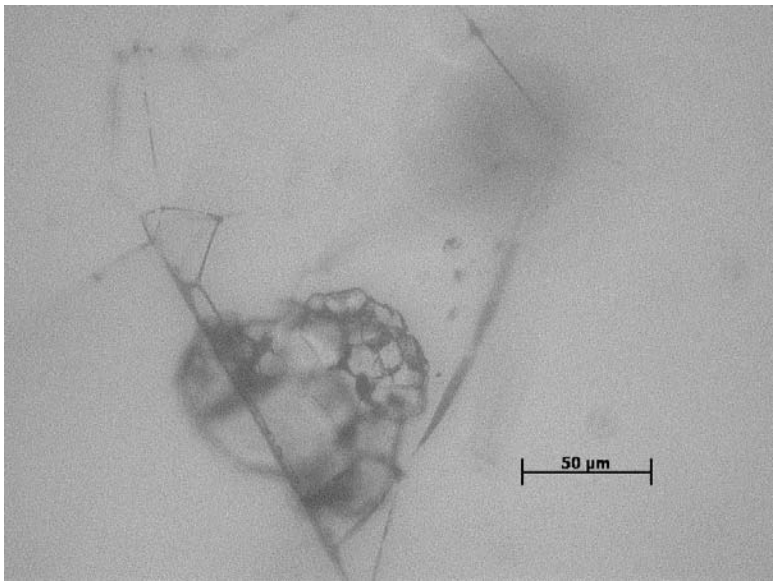

Figure 29. A single slice taken using transmitted brightfield at 500×. The gray on gray nature of the all the slices prevented even a projection rendering of stack.

The three phase illumination modes provide a good survey method to determine feature and grain boundary locations, but the diffraction patterns generated eliminate these modes for the required studies. Phase objectives do not possess the needed working depths, nor do they support the alternate techniques required on a regular bases.

8. Pending Issues

Most of the imaging issues are pending due to the random nature of their occurrence. Using a transmitted laser, image quality changed without warning as seen in the noise in figure 30 and were made a day apart using identical settings.

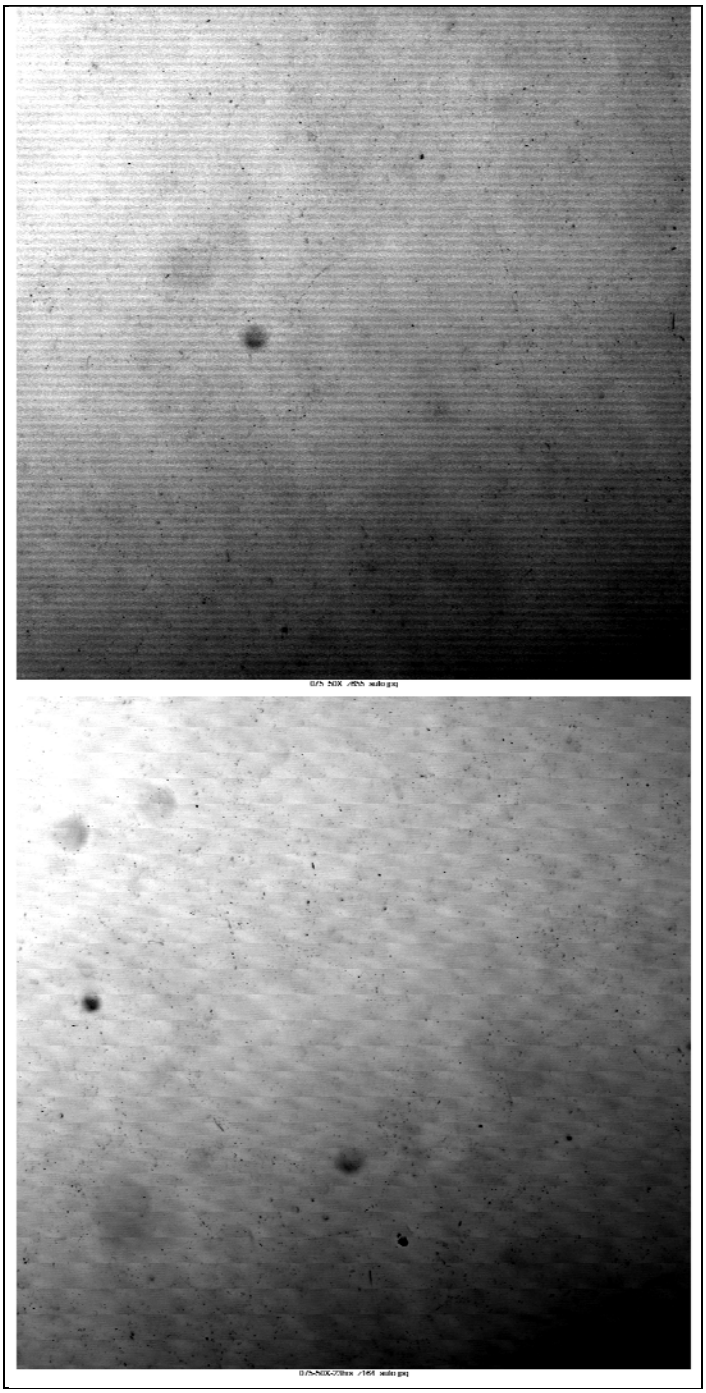

Figure 30. One of the random issues encountered. At top, the transmitted laser image is lined whereas in the bottom the image is normal. Both are from 8 h collections.

The broadband light level changes mid-frame as seen in figures 31 and 32 from one Z-stack collected using the charge-coupled device (CCD) camera and illustrate a more improbable problem.

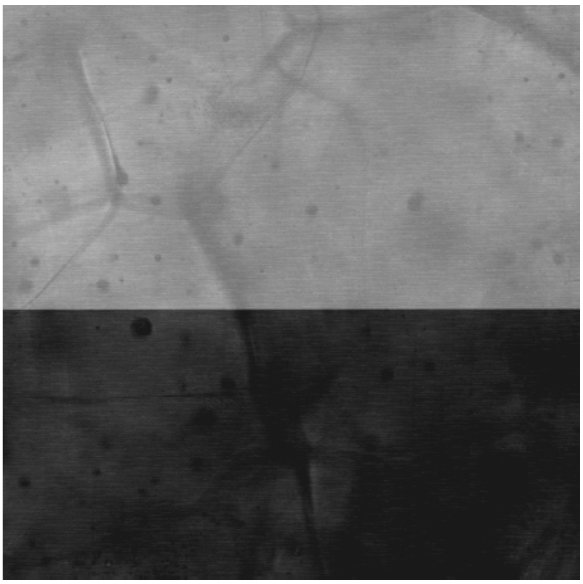

Figure 31. One of two slices from a CCD-generated Z-stack using light-emitting diode (LED) illumination. What changed at mid frame?

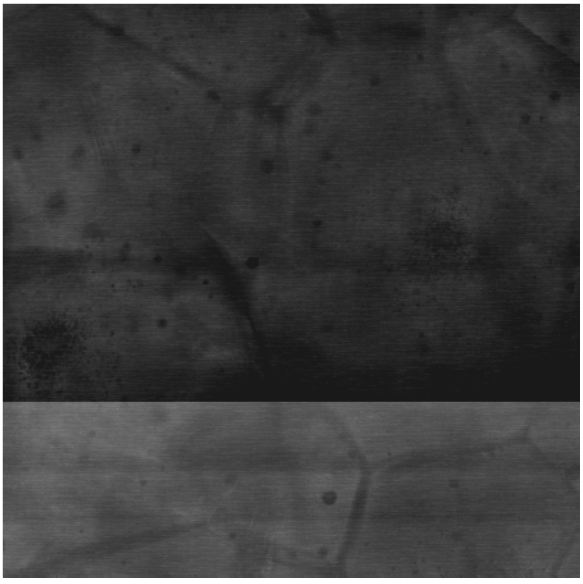

Figure 32. A variation of the figure 30 image issue. Capture time for both was 64 ms.

The processing applications are incapable of handling the bars shown earlier in figure 30 and the light level changes in figures 31 and 32. These issues appear to be unique to the hybrid Z1m, with the presence of the two Zeiss applications, and the fiber optic camera with video card.

The new Z2m, 64 bit AV4, and new application modules will address the present processing deficiencies, but the in situ multisurface imaging issue may need either the AV4 4D module, or a third party application. Quantization will only be possible with reliably reproducible Z-stacks and 3-D topographic results.

List of Symbols, Abbreviations, and Acronyms

3-D	three-dimensional
AlON	aluminum oxy nitride
AV4	AxioVision 4.x
CCD	charge-coupled device
C-DIC	Circular-Differential Interference Contrast
HIP	Hot Isostatic Pressing
LED	light-emitting diode
LSM	Zeiss Pascal software
$MgAl_2O_4$	magnesium aluminate
NIH	National Institutes of Health
Z1m	Zeiss Pascal 5 confocal microscope

NO. OF COPIES	ORGANIZATION
1 (PDF)	DEFENSE TECHNICAL INFORMATION CTR DTIC OCA
1 (PDF)	DIRECTOR US ARMY RESEARCH LAB IMAL HRA
1 (PDF)	DIRECTOR US ARMY RESEARCH LAB RDRL CIO LL
1 (PDF)	GOVT PRINTG OFC A MALHOTRA
1 (PDF)	DIR USARL RDRL WMM E D HARRIS

INTENTIONALLY LEFT BLANK.